

# High-Resolution Computed Tomography of Fibrotic Interstitial Lung Disease

Karen Rodriguez, MD<sup>1</sup> Christian L. Ashby, MD<sup>2</sup> Valeria R. Varela, MD<sup>2</sup> Amita Sharma, MD<sup>1</sup>

<sup>1</sup>Division of Thoracic Imaging and Intervention, Department of Radiology, Massachusetts General Hospital, Boston, Massachusetts  
<sup>2</sup>School of Medicine, Universidad Central del Caribe School of Medicine, Bayamón, Puerto Rico

Address for correspondence Amita Sharma, MD, Division of Thoracic Imaging and Intervention, Department of Radiology, Massachusetts General Hospital, Austen 202, 55 Fruit Street, Boston, MA 02114 (e-mail: Asharma2@mgh.harvard.edu).

Semin Respir Crit Care Med 2022;43:764–779.

## Abstract

### Keywords

- ▶ interstitial lung disease
- ▶ high-resolution computed tomography
- ▶ fibrosis
- ▶ traction bronchiectasis
- ▶ honeycombing
- ▶ fibrotic sarcoidosis

While radiography is the first-line imaging technique for evaluation of pulmonary disease, high-resolution computed tomography (HRCT) provides detailed assessment of the lung parenchyma and interstitium, allowing normal anatomy to be differentiated from superimposed abnormal findings. The fibrotic interstitial lung diseases have HRCT features that include reticulation, traction bronchiectasis and bronchiolectasis, honeycombing, architectural distortion, and volume loss. The characterization and distribution of these features result in distinctive CT patterns. The CT pattern and its progression over time can be combined with clinical, serologic, and pathologic data during multidisciplinary discussion to establish a clinical diagnosis. Serial examinations identify progression, treatment response, complications, and can assist in determining prognosis. This article will describe the technique used to perform HRCT, the normal and abnormal appearance of the lung on HRCT, and the CT patterns identified in common fibrotic lung diseases.

High-resolution computed tomography (HRCT) has become an indispensable tool in the diagnosis of fibrotic interstitial lung disease (ILD). Specifically, thin-section images and high spatial resolution allow for better characterization of altered anatomy patterns in ILD than plain radiographs.<sup>1,2</sup> Characteristic CT features may determine a fibrotic lung pattern with enough confidence to obviate the need for biopsy or direct the most appropriate biopsy site. Combined with clinical, pathologic, and serologic data, HRCT can direct the most appropriate management pathways, monitor therapies, and provide prognostic information.

### High-Resolution Computed Tomography Technique

The scanning protocol for the evaluation of diffuse lung disease includes single breath-hold, volumetric, thin-section imaging of the chest (1–1.5 mm thickness to minimize partial volume averaging), obtained at suspended full inspiration and reconstructed with a high-spatial frequency algorithm.<sup>1,3–6</sup> Interpretation using thick slices or expiratory images can lead to misdiagnosis of ILDs (▶ Fig. 1A, B). Supine

images are supplemented with volumetric or interspaced axial inspiratory prone images from the carina through the costophrenic angles. A common mimic of early fibrosis is gravity-dependent density, a normal physiological differential perfusion in the lungs, and posterior atelectasis that occurs when patients are scanned supine, particularly at reduced vital capacity (▶ Fig. 1C, D).<sup>7,8</sup> In both early fibrosis and dependent density, reticulation and ground-glass opacities occupy the typically empty posterior subpleural 1 cm of the lung on chest CT. Repeat scanning in a prone position results in resolution of posterior gravity-dependent opacities, but persistence of pathologic features (▶ Fig. 2A–D).<sup>6,9,10</sup> Additionally, nonvolumetric, axial interspaced expiratory supine images are performed from the apex to base to evaluate for air trapping. Most of the expected changes of ILD can be observed in the inspiratory phase, with the exception of air trapping (▶ Fig. 3A, B).<sup>3,11</sup>

Postprocessing of volumetric imaging data includes multiplanar reformatted images in the coronal and sagittal planes to aid in the assessment of lung volumes and

published online  
October 28, 2022

Issue Theme Chest Imaging; Guest Editors: Martine Remy-Jardin, MD, PhD, Ann N.C. Leung, MD, and David A. Lynch, MB BCH

© 2022. Thieme. All rights reserved. Thieme Medical Publishers, Inc., 333 Seventh Avenue, 18th Floor, New York, NY 10001, USA

DOI <https://doi.org/10.1055/s-0042-1755563>.  
ISSN 1069-3424.

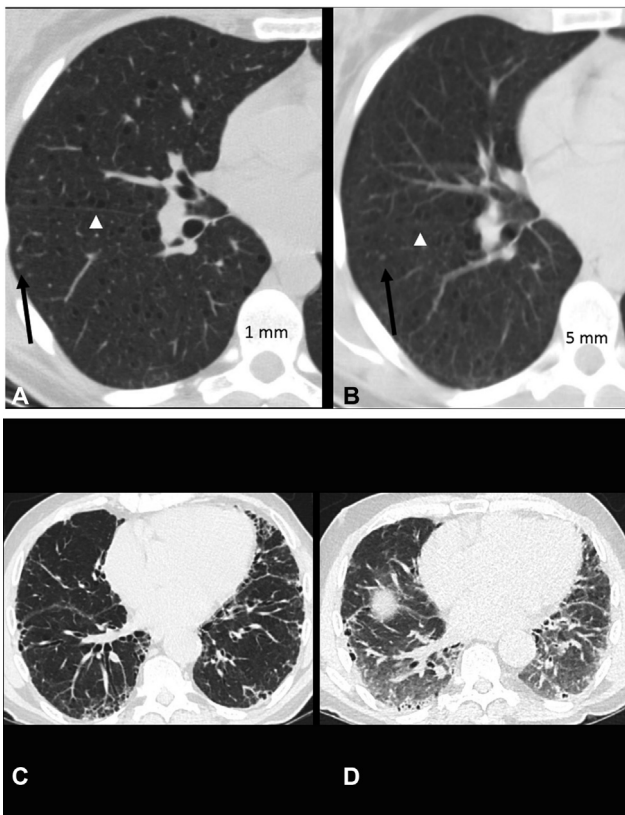


**Fig. 1** Technical considerations. Axial CT images in a patient with tuberous sclerosis. (A) 1-mm section demonstrates the right major fissure, thin-walled cysts from lymphangioleiomyomatosis (white arrowhead) and nodules from multifocal micronodular pneumocyte hyperplasia (black arrow) more sharply than the 5-mm section (B). Axial CT images in a patient with usual interstitial pneumonia pattern. Images in inspiration (C) compared with expiration (D) show decrease in lung volume and increase in attenuation of the lung on expiration, which can mimic additional abnormality.

distribution of disease.<sup>6,9</sup> Maximum and minimum intensity projection images improve detection of pulmonary nodules, traction bronchiectasis, and regions of low attenuation (► Fig. 4A, B).<sup>12</sup>

### Normal Anatomy

Structures as small as 0.2 mm can be identified on HRCT.<sup>13</sup> The smallest anatomic and functional unit of lung visible is the secondary pulmonary lobule (SPL; ► Fig. 5A, B). The SPL is polyhedral in shape, measures 1 to 2.5 cm in size, and contains 5 to 20 acini.<sup>13–15</sup> SPLs are separated by connective tissue interlobular septa that are only partially visible on CT, usually in the lung apices or bases, unless abnormally thickened.

The acini within the SPLs are supplied by a lobular bronchiole and the pulmonary artery that are centrilobular structures. The lobular bronchiole divides into terminal and respiratory bronchioles that open into the alveolar air sacs, where gas exchange occurs. The branches of the pulmonary arteries run alongside the airway and bring deoxygenated blood to the rich capillary network. Branches of the pulmonary vein run within the interlobular septum and return

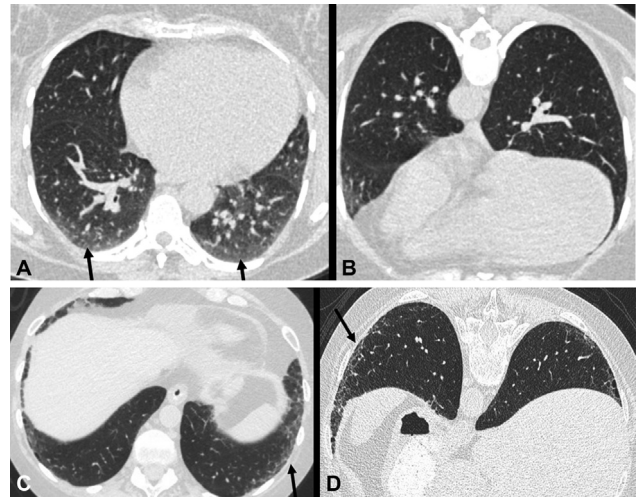


**Fig. 2** (A) Supine chest CT images demonstrate dependent density in the lung bases (arrows). (B) Prone CT image demonstrate resolution of the ground-glass opacities. (C) Supine axial CT images showing lower lobe subpleural reticulation (arrow). (D) Prone CT images show persistence of subpleural reticulations consistent with early fibrosis (arrow).

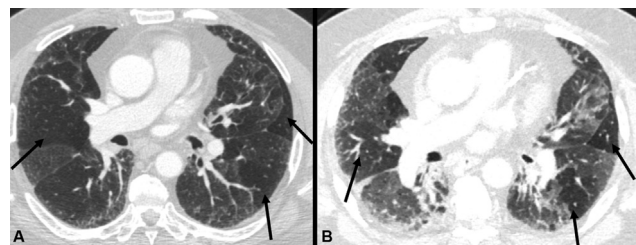


**Fig. 3** Air trapping in fibrotic hypersensitivity pneumonitis. Axial CT images in inspiration (A) demonstrate lobular lucencies (arrows). Persistence of volume and low attenuation in these areas on the expiratory study are consistent with air trapping (arrows, B). Regions of normal and increased attenuation on inspiration demonstrate decrease in volume and increase in attenuation on expiratory study.

oxygenated blood to the heart. The interstitium is the connective tissue framework that supports the lung.<sup>16</sup> It consists of the subpleural peripheral interstitium and interlobular septa, the axial interstitium that surrounds the bronchovascular bundles, and the intralobular interstitium, which radiates from the airway walls to surround the alveoli. The lymphatics lie within the axial and peripheral interstitium.

### Features of Fibrosis

HRCT features of fibrosis consist of irreversible reticulation, traction bronchiectasis, honeycombing, architectural distortion, and volume loss.

#### Reticulation

An early HRCT feature of fibrosis is irreversible and progressive reticulation, which consists of a network or mesh of fine and coarse linear opacities (► Fig. 6A, B). These irregular intersecting lines represent both interlobular septal thickening and intralobular interstitial thickening.<sup>13,14,17,18</sup>

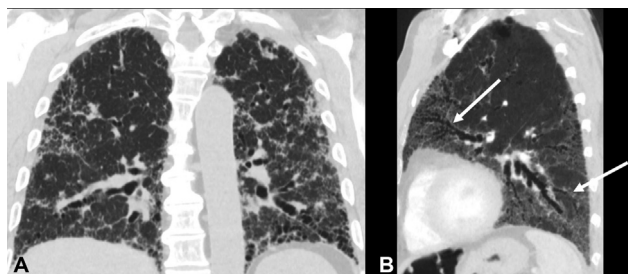


**Fig. 4** Postprocessing of volumetric data. (A) Coronal CT image in a patient with usual interstitial pneumonia demonstrates volume loss and lower lobe predominant subpleural reticulation, traction bronchiectasis, and basal honeycombing. (B) Sagittal minimum intensity projection images highlight traction bronchiectasis in the anterior upper lobe (arrow) and lower lobe (arrow) in a different patient with connective tissue disease interstitial lung disease.

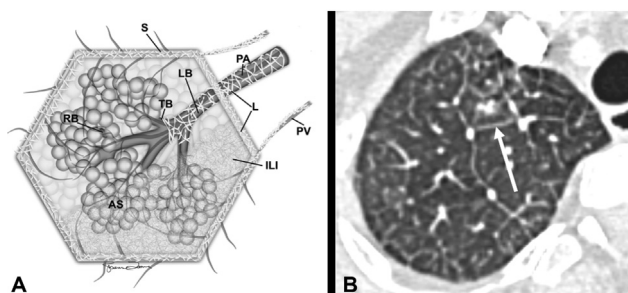


**Fig. 5** Diagrammatic representation of the secondary pulmonary lobule (SPL). (A) An SPL is surrounded by interlobular septa. Within the center of the SPL, a lobular bronchiole (LB) divides into several terminal bronchioles (TB) that in turn divide into multiple respiratory bronchioles (RB) which communicate with the alveolar sacs (AS). The pulmonary artery (PA) branches divide in the center of the SPL alongside the bronchioles. There is an internal framework of connective tissue within the SPL that surrounds the alveolar sacs, known as the intralobular interstitium (ILI). The lymphatics (L) lie within a sheath that surrounds the bronchovascular bundle and within the interlobular septa (S) together with the pulmonary vein (PV). (B) Axial CT of the right apex in patient with pulmonary edema demonstrating corresponding anatomy of the SPL outlined by the thickened interlobular septum (arrow).

Volume loss occurs due to alveolar collapse within the SPL, causing irregularity of the interlobular septum, distortion of the fissures, and irregular interfaces.<sup>13</sup> Ground-glass opacity within areas of reticulation and traction bronchiectasis, represented by increased lung attenuation with preservation of the vessel outline, is secondary to fine fibrosis beyond the resolution of HRCT.<sup>19</sup> Reticulation may also occur with inflammatory conditions that are reversible, so cannot be used alone as an indicator of fibrosis when other features are absent.<sup>20</sup>

### Traction Bronchiectasis

Traction bronchiectasis and bronchiolectasis represent irregular, irreversible airway dilatation caused by retractile pulmonary fibrosis.<sup>13</sup> Reticulation and ground-glass opacities are present adjacent to the dilated, varicose airways (–Fig. 7A, B). Identification of adjacent features of fibrosis helps differentiate this entity from standalone bronchiectasis, in which irreversible, localized, or diffuse dilatation of the

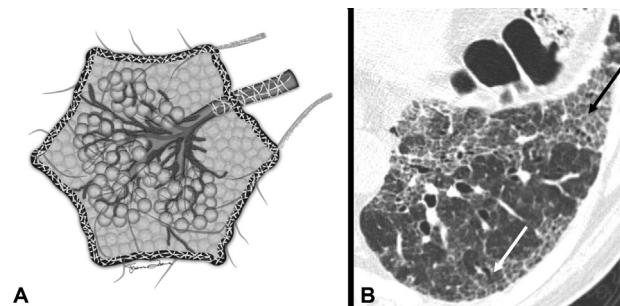


**Fig. 6** Reticulation. (A) Diagrammatic representation of reticulation. The secondary pulmonary lobule (SPL) demonstrates fine intralobular lines and ground-glass opacity secondary to thickening of the intralobular interstitium. There is irregularity of the interlobular septum and decreased volume of the SPL. (B) HRCT demonstrating thickening of the intralobular lines and ground-glass opacities (black arrow) secondary to fine fibrosis. Traction bronchiectasis is noted in this region (white arrow).

airway is secondary to infection, proximal airway obstruction, or a congenital bronchial abnormality (–Fig. 8A, B).<sup>13</sup> Traction bronchiolectasis is most apparent in the lung periphery, where the absence of cartilage in the distal airways enables mechanical traction, distortion, and dilatation.<sup>21</sup> Traction bronchiectasis predominates in the periphery of the lower lobes in usual interstitial pneumonia (UIP) and nonspecific interstitial pneumonia (NSIP) CT patterns, although those with NSIP may demonstrate subpleural sparing. Involvement of the central upper and mid-zones is associated with fibrotic hypersensitivity pneumonitis (HP) and sarcoidosis. Generally, traction bronchiectasis progresses slowly over months to years but can develop within days in acute interstitial pneumonia (AIP) and other forms of diffuse alveolar damage.<sup>22–24</sup> Walsh and colleagues reported good interobserver variability for the detection of traction bronchiectasis that exceeded agreement for honeycombing.<sup>25,26</sup> Tominaga et al demonstrated improved interobserver agreement for traction bronchiectasis when observers noted evidence of a surrounding fibrosing pneumonia and exclusion of bronchiectasis related to airway disease, consolidation, or a focal lesion.<sup>27</sup> Coexisting emphysema can reduce diagnostic confidence for honeycombing.<sup>28</sup> Traction bronchiectasis may be absent within regions of coexisting emphysema.<sup>29</sup> Destruction of the lung parenchyma may result in loss of the intralobular interstitial fibers that are responsible for the retractile fibrosis, which causes traction.

Traction bronchiectasis has both diagnostic and prognostic implications. The presence and severity of traction bronchiectasis has been shown to be an independent predictor of higher mortality irrespective of the HRCT pattern.<sup>21,29,30</sup>

### Honeycombing

This finding is the hallmark of end-stage fibrosis (–Fig. 9A, B). It results in a complete loss of the acinar architecture, resulting in cystic airspaces. Cystic airspaces measure between 3 and 3 cm in diameter and share relatively thick, well-defined walls.<sup>13</sup> Honeycomb cysts are peripheral and subpleural in location, can be multilayered or single layered, and are most often associated with traction bronchiectasis.<sup>13</sup>

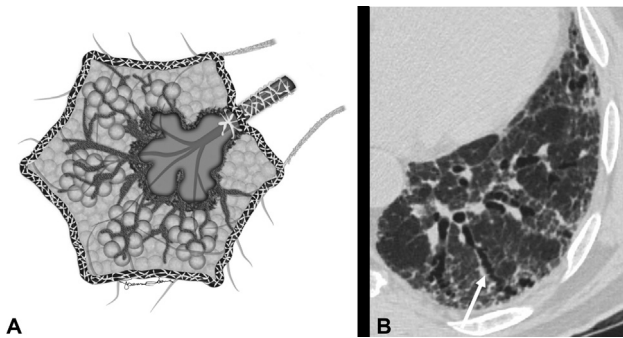


**Fig. 7** Traction bronchiectasis. (A) Diagrammatic representation of the secondary pulmonary lobule (SPL) demonstrates dilatation of the centrilobular bronchiole, traction bronchiectasis, and surrounding reticulation and ground-glass opacity. There is also irregular septal thickening which results in distortion and loss of volume of the SPL. (B) HRCT of the left lower lobe showing basal predominant reticulation adjacent to traction bronchiectasis (arrow).

While this is an important sign of fibrosis, studies have shown only moderate agreement in identifying honeycombing among radiologists.<sup>28,31</sup> Mimics of honeycombing on CT images include paraseptal emphysema, airspace enlargement with fibrosis, and traction bronchiectasis.<sup>13,20,21,28,31,32</sup> Paraseptal emphysema typically manifests as a single layer of thin-walled cystic spaces with intact interlobular septa; these are more common in the upper lobe rather than in the lower lobes (→Fig. 10A, B). They run along the pleural surface, fissure, and mediastinum. Importantly, there is no adjacent reticulation, ground-glass opacity, architectural distortion, or traction bronchiectasis in patients with paraseptal emphysema. Initially described only with idiopathic pulmonary fibrosis (IPF), honeycombing is also seen in patients with connective tissue disease (CTD)-related ILD, fibrotic HP, and sarcoidosis. In all these conditions, the extent of honeycombing is predictive of increased mortality.<sup>31,33</sup>



**Fig. 8** Differentiating traction bronchiectasis from standalone bronchiectasis. (A) Axial chest CT demonstrates traction bronchiectasis associated with subpleural reticulation and architectural distortion. (B) Axial chest CT demonstrates bronchiectasis secondary to prior infection. There is normal lung surrounding the bronchiectasis with no adjacent reticulation or ground-glass opacity.

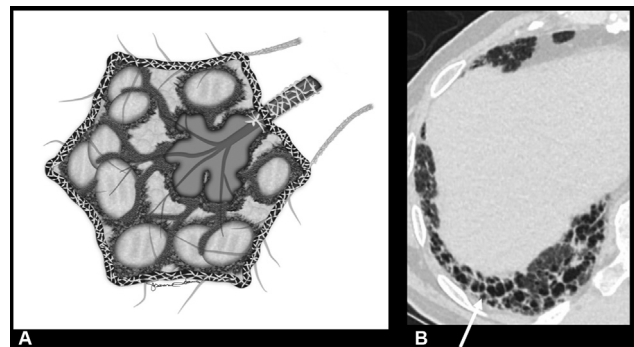


**Fig. 9** Honeycombing. (A) Diagrammatic representation of the secondary pulmonary lobule (SPL) demonstrates honeycomb cystic change. There is volume loss of the SPL associated with irregular septal thickening and cysts. Traction bronchiectasis is also present. (B) HRCT findings showing right lower lobe basal predominant honeycombing (arrow).

**Architectural Distortion**

Architectural distortion of the lung parenchyma refers to displacement of the bronchi, pulmonary vessels, and fissures associated with irregular interfaces at pleural surfaces.<sup>31,34–36</sup> Architectural distortion and volume loss are associated features of fibrosis (→Fig. 11A, B).

**Computed Tomography Patterns of Fibrosis**

The process of HRCT evaluation involves identification and characterization of abnormal findings at the level of the SPL and assessment of distribution of disease in the craniocaudal and axial planes. This allows radiologists to identify specific CT patterns that correspond to morphologic pathologic patterns.<sup>37,38</sup> The CT pattern, clinical presentation, and serologic data are optimally reviewed during a multidisciplinary discussion between radiologists, pulmonologists, pathologists, and rheumatologists to formulate a working clinical diagnosis of ILD and assess the need for lung biopsy. Initial diagnoses may change in up to half of challenging cases following multidisciplinary discussion.<sup>39,40</sup> Repeated discussion is helpful as CT patterns, clinical symptoms, and serology may evolve.<sup>41</sup>

The main CT patterns associated with the fibrotic ILDs include UIP, NSIP, fibrotic organizing pneumonia (OP), fibrotic HP, and fibrotic sarcoidosis. The American Thoracic Society (ATS) and the European Respiratory Society (ERS) consensus panel subclassified chronic fibrosing interstitial

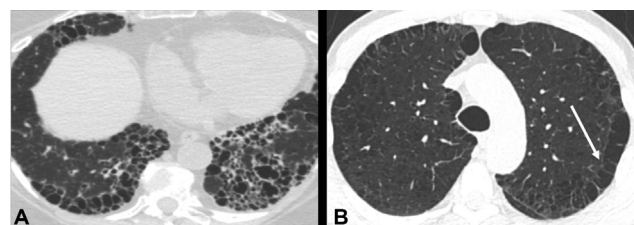


**Fig. 10** Mimics of honeycombing. (A) Axial HRCT demonstrates lower lobe honeycombing. (B) HRCT with single layer of thin-walled cystic spaces with intact interlobular septa consistent with paraseptal emphysema (arrow).

This document was downloaded for personal use only. Unauthorized distribution is strictly prohibited.

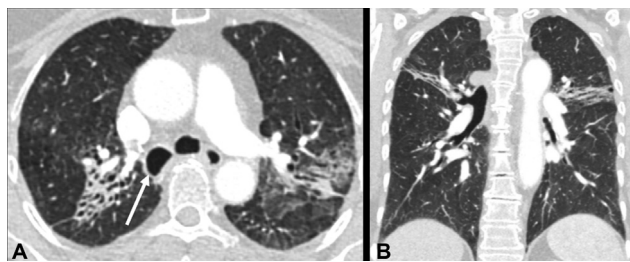


**Fig. 11** Architectural distortion in fibrotic sarcoidosis. (A) Axial and (B) coronal chest CTs demonstrate architectural distortion, traction bronchiectasis, and linear densities radiating from hila. Crowding of the airways and vessels and volume loss in the posterior upper lobe are associated with posterior displacement of the right main bronchus (arrow).

pneumonias as either idiopathic or of known etiology.<sup>42</sup> Currently, only four of these clinical syndromes—IPF, NSIP, cryptogenic organizing pneumonia (COP), and pleuroparenchymal fibroelastosis (PPFE)—are considered idiopathic.<sup>43,44</sup> Other interstitial pneumonias with known etiologies include CTD-associated ILD, HP, and sarcoidosis.<sup>45,46</sup> The most common fibrotic ILD is IPF, characterized by a histologic or radiologic UIP pattern.

### Usual Interstitial Pneumonia

The CT-UIP pattern is characterized by reticulation, honeycombing, and traction bronchiectasis in a basal and subpleural distribution<sup>1,42</sup> (►Fig. 12A, B). This predicts a histologic UIP pattern with a positive predictive value of 90 to 100%.<sup>32</sup> Given the high concordance between CT-UIP and path-UIP, CT-UIP obviates the need for lung biopsy.<sup>30</sup> Identification of a CT-UIP pattern is of primary importance due to its association with the clinical syndrome of IPF.<sup>41</sup> However, a CT-UIP pattern is also seen in CTDs, fibrotic HP, occupational or medication exposure, familial fibrosis, and rarely sarcoidosis. Ancillary clues to these causes may be present on chest CT within the mediastinum, pleura, and bones. These include mediastinal lymphadenopathy in sarcoidosis, esophageal dilatation in scleroderma, pleural effusion, thickening, or plaques to suggest CTD or asbestos exposure and bony erosions, such as seen with rheumatoid arthritis. Careful clinical and serologic exclusion of secondary causes is needed before attributing a CT-UIP pattern to IPF. Age over 60 years, male gender, and smoking history are parameters favoring IPF as the most likely diagnosis of a CT-UIP pattern.<sup>47,48</sup>

In 2018, the ATS/ERS/Japanese Respiratory Society (JRS)/Asociación Latinoamericana del Tórax (ALAT) and the Fleischner Society separately released updated guidelines for diagnosing IPF.<sup>1,42</sup> Previous guidelines had described three different CT patterns for patients suspected of having IPF: UIP, possible UIP, and inconsistent with UIP patterns.<sup>49</sup> A shortcoming of three CT categories became apparent. Although a CT-UIP pattern is highly specific for IPF in the correct clinical context, up to 60% of patients with histologically proven UIP and clinical diagnosis of IPF do not have a CT-UIP pattern due to the lack of honeycombing.<sup>50–53</sup> This significant proportion of IPF patients would be categorized

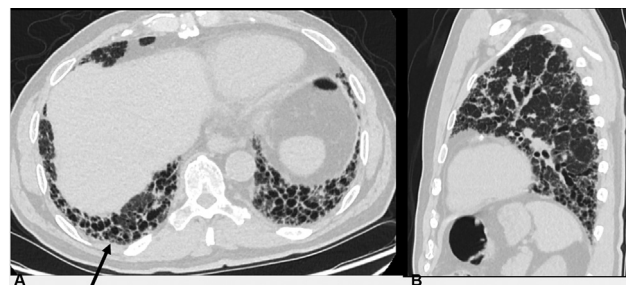


**Fig. 12** A 69-year-old male with usual interstitial pneumonia pattern. (A) Axial HRCT shows basal predominant honeycombing (arrow). (B) Sagittal CT image highlights traction bronchiectasis and honeycombing in a basal and subpleural distribution.

on CT as possible UIP, for which lung biopsy was recommended. In a population that was frail and elderly, the inability to obtain tissue failed to classify patients and offer antifibrotic therapy accurately. The 2018 ATS/ERS/JRS/ALAT updated recommendations, as well as the Fleischner Society White Paper on Diagnostic Criteria for IPF, now describe four CT patterns: UIP, probable UIP, indeterminate for UIP, and findings that suggest an alternative diagnosis to IPF/CT features most consistent with a non-IPF diagnosis<sup>42</sup> (►Table 1).

The CT patterns described in both guidelines are essentially similar (►Fig. 13). The CT-UIP pattern is characterized by reticulation, honeycombing, and traction bronchiectasis in a basal and subpleural distribution, although the distribution may be diffuse, patchy, or asymmetric (►Fig. 13A). Patients with a probable UIP pattern have no evidence of honeycombing but display reticular abnormalities with peripheral traction bronchiectasis or bronchiectasis in a basal and subpleural-predominant distribution (►Fig. 13B).<sup>42</sup> Studies have reported that a probable UIP pattern is associated with histological UIP or probable UIP in 80 to 94% of cases. A study by Shih et al that assessed the practical application of both 2018 guidelines found that typical UIP and probable UIP on CT had high specificity for histopathologic UIP.<sup>49</sup> However, the positive predictive value of CT probable UIP was lower than reported elsewhere and further studies are required.<sup>49,53,54</sup>

The indeterminate for UIP-CT pattern category includes patients who do not fit the criteria for a typical UIP pattern or a probable UIP pattern and instead display a more diffuse distribution, ground-glass opacities, and reticulation without any other features of fibrosis (►Fig. 13C).<sup>42</sup> A study by Chung and colleagues found that pathologic UIP was seen in 82 and 54% of cases with probable UIP on CT and indeterminate pattern, respectively.<sup>54</sup>

An upper or mid-zone or peribronchiolar distribution, subpleural sparing, or the presence of predominant ground-glass or consolidative opacities, mosaic attenuation, diffuse nodules, or cysts are classified as an alternative diagnosis to IPF and should be evaluated for another cause (►Fig. 13D). The only exception is when diffuse ground-glass opacities are superimposed on a typical UIP pattern and may indicate acute exacerbation of IPF (►Fig. 14). Mosaic attenuation

**Table 1** Diagnostic categories of UIP based on CT patterns

	Typical UIP-CT pattern	Probable UIP-CT pattern	CT pattern indeterminate for UIP	CT features most consistent with non-IPF diagnosis
CT distribution	Basal (occasionally diffuse) and subpleural predominant. Distribution is often heterogeneous	Basal and subpleural predominant. Distribution is often heterogeneous	Variable or diffuse	Upper or mid-lung predominant fibrosis peribronchovascular predominance with subpleural sparing
CT features	Honeycombing. Reticular pattern with peripheral traction bronchiectasis/bronchiolectasis. <sup>a</sup> Absence of features to suggest an alternative diagnosis	Reticular pattern with peripheral traction bronchiectasis/bronchiolectasis. <sup>a</sup> Honeycombing is absent	Evidence of fibrosis with some inconspicuous features suggestive of non-UIP pattern <sup>a</sup>	Any of the following: Predominant consolidation. Extensive pure ground-glass opacity (without acute exacerbation) Extensive mosaic attenuation with extensive sharply defined lobular air trapping on expiration Diffuse nodules or cysts

Abbreviations: CT, computed tomography; IPF, idiopathic pulmonary fibrosis; UIP, usual interstitial pneumonia.

Source: Reprinted with permission from Lynch et al.<sup>1</sup>

<sup>a</sup>Reticular pattern is superimposed on ground-glass opacity, and, in these cases, is usually fibrotic. Pure ground-glass opacity, however, would be against the diagnosis of UIP/IPF and would suggest acute exacerbation, hypersensitivity pneumonitis, or other conditions.

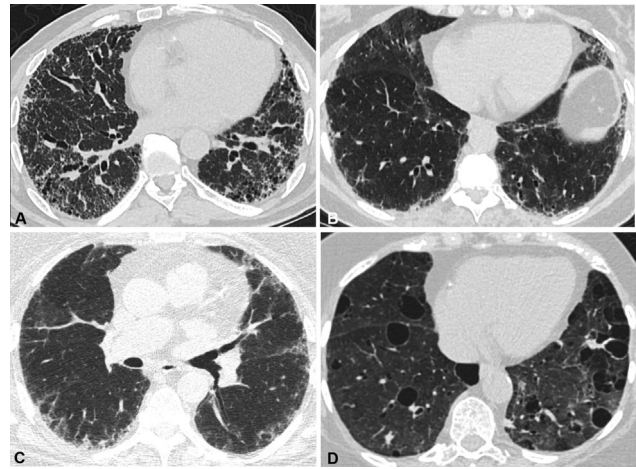


**Fig. 13** Diagnostic categories of usual interstitial pneumonia (UIP). (A) Typical UIP-CT pattern. HRCT demonstrates basal predominant subpleural reticulation with peripheral traction bronchiectasis and honeycombing. (B) Probable UIP-CT pattern. Basal predominant subpleural reticulation with peripheral traction bronchiectasis without honeycombing. (C) Indeterminate UIP-CT pattern. HRCT demonstrates reticulation with inconspicuous features suggestive of non-UIP pattern. (D) CT features most consistent with non-idiopathic pulmonary fibrosis diagnosis. HRCT demonstrates multiple cysts from lymphocytic interstitial pneumonia in a patient with Sjogren's syndrome.

raises the possibility of fibrotic HP, but air trapping in regions of the fibrotic lung is also frequently identified in IPF.<sup>50,55</sup>

The ATS/ERS/JRS/ALAT revised guidelines conditionally recommend performing bronchoalveolar lavage (BAL) and surgical biopsy on patients with features of probable UIP pattern, indeterminate for UIP pattern, or findings associated with an alternative diagnosis.<sup>42</sup> However, the recommendation for surgical lung biopsy in patients with probable UIP is conditional and not mandatory for diagnosing UIP/IPF in patients with a clear clinical context.

The Fleischner Society revised guidelines support the role of CT for the diagnosis of IPF, without the need for surgical tissue sampling, in the context of both typical and probable UIP patterns.<sup>1</sup> In patients with suspected IPF but unclear clinical context and no definite or probable UIP pattern on CT, a biopsy may be considered to confirm or exclude a diagnosis of UIP.<sup>1</sup>

HRCT scanning patterns may predict clinical outcomes in patients with IPF. Flaherty et al found that typical UIP pattern on HRCT was predictive of a worse prognosis in patients with IPF compared to patients with an atypical pattern.<sup>56</sup> A study by Kwon et al found that IPF patients with a probable UIP pattern, and those with a definite UIP pattern, had similar prognosis and patients with an indeterminate UIP pattern demonstrated a lesser decline in lung function and a higher survival rate compared to those who were compared to other scanning patterns in IPF patients.<sup>57,58</sup> Comparably, Fukihara et al found no significant survival difference between patients with probable UIP and definite UIP patterns on HRCT.<sup>59</sup>

On the other hand, Salisbury et al found that patients with a possible UIP pattern had a more prolonged disease-free

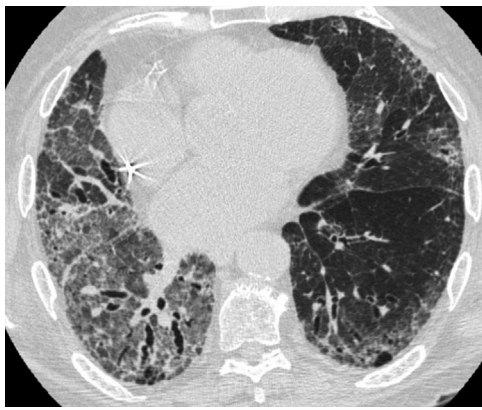


**Fig. 14** Acute exacerbation of interstitial lung disease. HRCT demonstrates multifocal ground-glass opacities primarily in the right lower lobe superimposed on a background of subpleural reticulation and traction bronchiectasis.

survival than patients with a definite UIP pattern.<sup>60</sup> Mononen et al found that the extent of traction bronchiectasis correlated with shortened survival for patients with IPF.<sup>61</sup> This study reported a more prolonged survival for patients with possible UIP compared to patients with definite UIP and found that evidence of honeycombing and architectural distortion is associated with shortened survival.<sup>61</sup> Additionally, lung parenchymal abnormalities on initial HRCT may predict lung function decline and may be independently predictive of prognosis in patients with biopsy-confirmed fibrotic idiopathic interstitial pneumonias (IIPs).<sup>62</sup> Lee et al showed that the extent of ground-glass opacities seen on the initial HRCT is negatively correlated with change in vital functional capacity (FVC) at follow-up.<sup>62</sup>

In terms of the progression of the disease, a study by Salvatore et al intended to determine patterns of progression in patients with probable UIP patterns.<sup>63</sup> They reviewed clinical information for 103 patients with a working diagnosis of IPF. They found that among patients with an initial diagnosis of probable UIP, 47% of them progressed to a definite diagnosis of UIP.<sup>63</sup> This cohort's median time of progression was 51 months.<sup>63</sup> They also reported that honeycombing was at least twice more likely to progress in patients with baseline emphysema.<sup>63</sup> Interestingly, they found a significant association between pulmonary artery size and an elevated risk for advanced progression of honeycombing.<sup>63</sup> Finally, Lee et al studied serial changes of lung abnormalities on HRCT in patients with a histologic diagnosis of a fibrotic IIP with little honeycombing.<sup>62</sup> They found that during a follow-up period of at least 2 years, the overall extent of reticulation and honeycombing increased for patients with UIP, while the extent of ground-glass opacification decreased (► **Fig. 15A, B**).<sup>62</sup>

IPF has a poor prognosis with a mean survival of 2.5 to 3.5 years from diagnosis if left untreated.<sup>42,64</sup> Early diagnosis guides antifibrotic treatment which reduces the decline in pulmonary function.<sup>1,42,65,66</sup> Balestro et al studied HRCT changes over time in patients undergoing IPF treatment.<sup>67</sup> The investigators found that while treatment did indeed slow down lung function decline, the extent of honeycombing

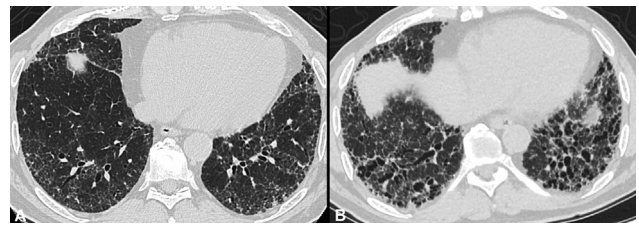


**Fig. 15** Progression of usual interstitial pneumonia over time. (A) HRCT demonstrates basal predominant subpleural reticulation with peripheral traction bronchiectasis and mild honeycombing. (B) Progression of traction bronchiectasis, honeycombing, and volume loss occur over a 4-year period.

continued to increase during the study period.<sup>67</sup> The study also showed a statistically significant correlation between the combined score of fibrosis (as measured by the interstitial score and the honeycombing) and the FVC decline.<sup>67</sup> Iwasawa et al supported the utility of CT to evaluate pirfenidone treatment response.<sup>68</sup> They found that in IPF patients undergoing pirfenidone therapy, the decline in vital capacity correlated with change in fibrosis and was significantly smaller in the pirfenidone group than in the control group when assessed by both a visual score and a computer analysis.<sup>68</sup>

Follow-up imaging is equally important to assess disease progression, treatment response, and disease complications. Radiologists may evaluate images using a subjective (semi-quantitative) assessment method in which a visual scoring system is used to measure the extent of fibrosis.<sup>48</sup> Jacob et al found that using a visual scoring system to quantify traction bronchiectasis severity predicted mortality independent of antifibrotic treatment and baseline disease severity.<sup>69</sup> Objective (quantitative) machine learning techniques are being evaluated to measure areas of healthy and fibrotic lung at thin-section CT.<sup>70</sup>

### Nonspecific Interstitial Pneumonia

NSIP is one of the most common histopathologic and radiologic patterns seen in patients with ILD.<sup>45,56,71</sup> When defining the CT features of NSIP, the 2008 ATS Working Group established a set of radiologic diagnostic characteristics that would be shared by both NSIP as an idiopathic disease and NSIP as a secondary finding.<sup>45,72</sup>

On HRCT, the most common findings include bilateral lower lobe predominant and symmetrically distributed ground-glass opacities accompanied by traction bronchiectasis (► **Fig. 16A, B**).<sup>42,45,72-76</sup> These findings typically have a unique lower-lung predominance, but parenchymal abnormalities can also occur in the upper lobes to a lesser extent.<sup>42,45,56,72,74,77</sup> NSIP may demonstrate relative sparing of the subpleural space, allowing differentiation from UIP.<sup>1,42,78,79</sup> Honeycombing is rarely seen in patients with NSIP.<sup>1,42,56,80</sup> Aside from the absence of honeycombing, NSIP can also be distinguished from UIP by its uniform spatial and temporal progression.<sup>45</sup>

Over time, the ground-glass opacities may be replaced by coarse reticulation, resulting in a CT pattern similar to the probable UIP pattern.<sup>1,78,81</sup> NSIP may also show some

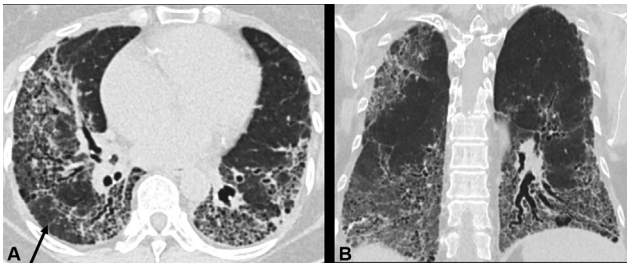


**Fig. 16** Fibrotic nonspecific interstitial pneumonia. (A) Axial HRCT and (B) coronal minimum intensity projection images. CT images demonstrate lower lobe predominant reticulation and traction bronchiectasis with subpleural sparing (arrow) and absence of honeycombing.

overlap with fibrosing OP with fibrosis in the lower lobes in a peribronchial distribution and subpleural sparing.<sup>1,82,83</sup>

Aside from imaging, NSIP also has unique clinical characteristics. The most significant difference is its better prognostic nature compared to patients with an identifiable UIP pattern<sup>84–86</sup> and those with IPF.<sup>42,84,87</sup> In fact, not only does NSIP carry a low mortality rate, but Katzenstein and Fiorelli noted that 83% of the patients involved in their study, even those who presented with severe fibrotic features, remained alive or recovered altogether.<sup>77</sup> The results of the ATS 2008 NSIP case series paralleled these findings and determined that the 5-year survival rate of patients with NSIP is 80%, while the 10-year survival rate is 73%.<sup>72</sup>

NSIP has a well-established connection with CTD, and it is rarely idiopathic. Patients who present with NSIP in the context of an underlying autoimmune disease, such as CTD, typically present with better outcomes than those with idiopathic NSIP, although the specific reasons are not currently understood.<sup>88–90</sup> Patients with NSIP also demonstrate differences in prognosis depending on the stage of the disease. A study performed by Latsi et al found that a histopathologic confirmation of a diagnosis of NSIP remained a predictor of mortality 6 months after the initial diagnosis and serial trends in pulmonary function indices. However, the reliability of this marker dwindled 12 months after the diagnosis, with serial pulmonary function tests being the only prognostic determinant.<sup>91</sup> A similar study performed by Jegal et al paralleled these findings. It concluded that although a histologic diagnosis of NSIP is prognostic of the long-term changes in lung function, after 6 months, FVC, diffusion capacity at diagnosis, and sex are the only reliable measures of short-term prognosis.<sup>92</sup>

### Organizing Pneumonia/Nonspecific Interstitial Pneumonia—Nonusual Interstitial Pneumonia

The relationship between OP and NSIP is not entirely understood, but OP is a common histologic finding in patients with NSIP. Additionally, patients with OP may progress to a pattern of NSIP on imaging (→**Fig. 17A, B**).<sup>29,33</sup> Patients treated for OP may still present on follow-up imaging with findings such as GGO and reticulation.<sup>33</sup> In addition, areas of fibrosis may become more conspicuous.<sup>29</sup> This residual fibrosis is lower-lobe predominant, has a peribronchial

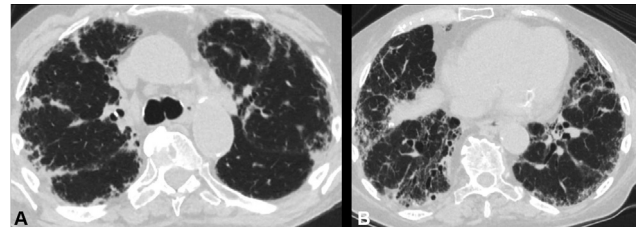


**Fig. 17** Organizing pneumonia/nonspecific interstitial pneumonia—non-usual interstitial pneumonia pattern. (A) HRCT demonstrate mid- and lower lung predominant subpleural consolidations. (B) HRCT in lower lobes demonstrates reticulation and traction bronchiectasis.

distribution, and demonstrates subpleural sparing—a pattern associated with NSIP.

### Acute Interstitial Pneumonia

AIP is an acute, rapidly progressive type of IIP associated with fulminant respiratory failure.<sup>93</sup> Exclusion of other lung diseases and absence of an identifiable cause or predisposing condition are prerequisites to diagnosis.<sup>22</sup> Diffuse alveolar damage is the key finding on histology and HRCT features depend on the timing of the disease.<sup>22,23</sup> Early in the disease course, an exudative phase is histologically characterized by edema in the interstitium and alveolus.<sup>22</sup> HRCT depicts symmetrical and bilateral, diffuse, or patchy ground-glass opacities and air space consolidations (→**Fig. 18**).<sup>22,23</sup> As the disease progresses, there is an organizing phase in which there is evidence of fibroblastic proliferation and type II pneumocyte hyperplasia.<sup>22,23</sup> The organizing phase is apparent within 5 to 7 days and characterized on HRCT by findings associated with fibrosis, distortion of bronchovascular bundles, traction bronchiectasis, architectural distortion, and interlobular septal thickening.<sup>22–24</sup> Extent of fibrosis on HRCT is an independent predictor of poor prognosis.<sup>24</sup>

### Idiopathic Pleuroparenchymal Fibroelastosis—Nonusual Interstitial Pneumonia

Among the fibrotic ILDs, idiopathic PPFE is both the rarest and most recently described.<sup>17</sup> The condition was first defined in a 2013 case series that described a group of patients with dense fibrosis of the visceral pleura and the subjacent lung parenchyma in the upper lobes, with a striking apical lung predominance.<sup>34</sup> While many cases of PPFE are idiopathic or familial, others have been associated with bone marrow and lung transplant, chemotherapy, chronic HP, prior pulmonary infection, and autoimmune diseases.<sup>94–101</sup> Prompt recognition of early radiological features is vital as patients with PPFE may rapidly undergo clinical deterioration.<sup>102</sup>

Fibrosis of the apical visceral pleura and fibroelastic changes within the subpleural lung parenchyma are key histologic features of PPFE depicted on HRCT (→**Fig. 19A, B**).<sup>100,102,103</sup> HRCT identifies small, dense pleural and subpleural consolidations with a reticular pattern, upper lobe volume loss, architectural distortion, traction bronchiectasis, parenchymal retraction, and upward displacement of hila.<sup>45,96,100,102,104,105</sup> Lower lobe involvement occurs as the disease progresses, leading to diaphragmatic elevation.





**Fig. 18** Acute interstitial pneumonia. Axial HRCT demonstrates diffuse ground-glass opacity and traction bronchiectasis, the latter developing 5 days after presentation.

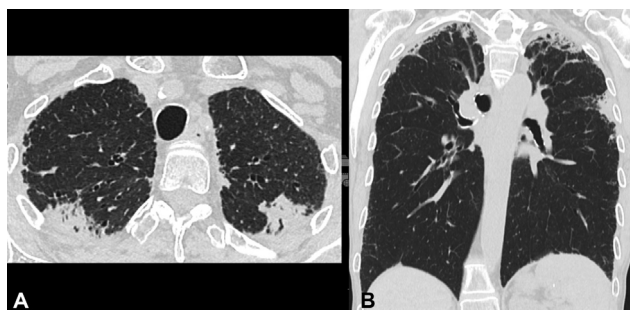


**Fig. 19** Pleural-parenchymal fibroelastosis. (A) Axial and (B) coronal chest CTs demonstrate upper lobe volume loss, peripheral consolidation, traction bronchiectasis, and architectural distortion.

Large cysts and bullae can be seen in the upper lobes with increased incidence of pneumothorax.<sup>101,105,106</sup>

Reddy et al defined cases as “definite” PPFE or “consistent” with PPFE.<sup>105</sup> In “definite” PPFE marked upper lobe involvement with pleural thickening and associated subpleural fibrosis is present. Cases “consistent” with PPFE similarly display upper lobe features with either involvement of lower lobes or features of coexistent lung disease.<sup>105</sup>

Patients with PPFE have a progressive restrictive pulmonary function decline that may be refractory to medical treatment.<sup>107</sup> Bilateral lung transplantation is considered the only therapeutic alternative though relapse after lung transplantation is possible.<sup>107</sup>

Recipients of lung and bone marrow transplants have developed PPFE after the transplant. Ofek et al found evidence of diffuse alveolar damage and bronchiolitis obliterans occurring concurrently with PPFE in patients following lung transplantation.<sup>108</sup>

### Sarcoidosis

Pulmonary fibrosis is seen in up to 20% of patients with sarcoidosis and is associated with increased mortality and morbidity due to respiratory failure.<sup>109,110</sup> The pathophysiology of fibrosis is due to a combination of persistent, unremitting granulomatous inflammation, profibrotic genetic features, and immune mechanisms.<sup>109</sup>



**Fig. 20** Fibrotic sarcoidosis. (A) Axial and (B) coronal chest CTs demonstrate coalescent central fibrosis in the bilateral upper lobes with volume loss and architectural distortion. There is peripheral cicatricial emphysema. The main bronchi are displaced posteriorly (asterisks).

HRCT can depict early parenchymal abnormalities and allows differentiation of active inflammation from irreversible fibrosis.<sup>111</sup> Distribution of fibrotic and nonfibrotic sarcoidosis are perilymphatic and in the upper and mid-zone.<sup>112</sup>

As with other fibrotic diseases, features include reticular opacities, architectural distortion, traction bronchiectasis, and volume loss.<sup>113,114</sup> HRCT demonstrates features of fibrosis extending from the hila as linear irregular densities, bronchiectasis, or conglomerate masses (→**Fig. 20A, B**). Volume loss, specifically in the posterior segment of the upper lobes, leads to posterior displacement of the upper lobe bronchi.<sup>115,116</sup> Peripheral paracicatricial emphysema (areas of lung overinflation adjacent to scarring) and large honeycomb cysts or bulla extend beyond the fibrosis.<sup>113,114</sup>

Verleden and colleagues correlated histopathologic features to CT and micro-CT of explanted lungs in patients with end-stage sarcoid and identified three main patterns.<sup>117</sup> Firstly, central fibrotic masses were associated with compression and obstruction of the centrilobular airways, loss of small airways, and architectural distortion. A second pattern of diffuse bronchiectasis was associated with septal thickening and upper lobe subpleural fibrosis. Finally, a third pattern, seen in only one patient, demonstrated a lower lobe UIP pattern. Other explant studies have reported that a subset of patients with fibrotic sarcoidosis display a UIP pattern.<sup>118,119</sup>

Abehsera and colleagues correlated HRCT findings with different functional profiles.<sup>120</sup> Evidence of a bronchial distortion pattern was associated with an obstructive ventilatory defect; a honeycombing pattern, on the other hand, was associated with restriction.<sup>115,120</sup> Handa and colleagues also found peribronchovascular thickening was associated with airflow limitation.<sup>110</sup>

Pulmonary hypertension is a complication of sarcoidosis and considered a predictor of poor clinical outcomes.<sup>121,122</sup> Pulmonary arteries are commonly involved by granulomas and may become obliterated by active inflammation and fibrosis, contributing to the development of pulmonary hypertension.<sup>122,123</sup> Walsh and colleagues validated an algorithm that combined a composite physiologic index with HRCT extent of lung fibrosis and pulmonary hypertension, measured as the ratio of the main pulmonary artery diameter to the diameter of the ascending aorta, to predict outcome and mortality.<sup>124</sup> Fibrosis greater than 20% was prognostic.

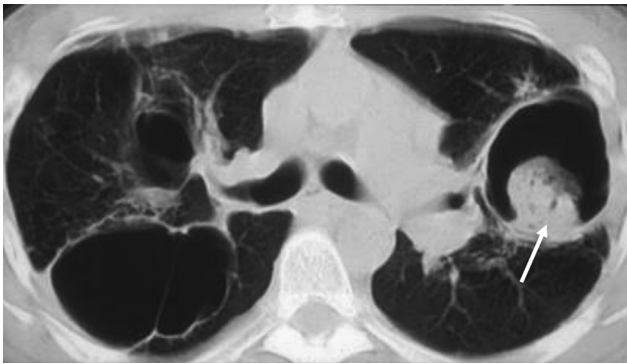


**Fig. 21** Axial chest CT in a patient with fibrotic sarcoidosis demonstrates large bullae and architectural distortion in the upper lobes. There is a cavitary mass in the left upper lobe representing a mycetoma (arrow).

In fibrotic sarcoidosis, acute exacerbations and pulmonary venous-occlusive disease are reported.<sup>125</sup> Cystic areas in fibrotic sarcoidosis may be colonized by aspergillomas, which are identified as intracavitary, mobile, enlarging nodular soft tissue, associated with adjacent pleural thickening (► Fig. 21).

**Hypersensitivity Pneumonitis**

HP is considered an immune-mediated reaction to inhaled organic and inorganic antigens in a sensitized individual. In up to 60% of cases, no inciting antigen is identified,<sup>126–130</sup> contributing to a widely varying registry prevalence of HP (2–47%) among patients with ILD.<sup>131–141</sup> There is also overlap between the presentation of HP and other fibrotic ILDs, leading to misdiagnosis and delayed management.<sup>142–146</sup> Although previously categorized based on symptom duration at the time of presentation (i.e., acute, subacute, or chronic),<sup>147,148</sup> inconsistency is reported in the outcomes of these subgroups; the natural history may include anything from progressive improvement to respiratory failure and over half of HP patients present with fibrosis.<sup>127,149–151</sup>

Two recently published guideline statements provide long-anticipated reclassification and algorithm-driven diagnostic approaches to HP. The ATS/JRS/ALAT guidelines<sup>11</sup> and Chest guidelines<sup>152</sup> recommend that HP should be subclassified based simply on the presence or absence of histologic or radiologic evidence of fibrosis, as fibrosis has implications for treatment and prognosis. Both guidelines stress that HRCT is integral to the diagnosis of HP but cannot be used alone to make the diagnosis, particularly in the absence of a known inciting antigen. While there are important differences between the two guidelines, their principles on the role of imaging are similar. Two groups of imaging descriptors are described. The first set classifies the HRCT pattern as either nonfibrotic HP or fibrotic HP. The second set provides a summary of the HRCT findings, categorizing fibrotic HP as “typical HP” when highly suggestive, “compatible with HP” when findings are less frequently reported but compatible, and “indeterminate of HP” when findings are not suggestive of HP, but do not exclude the diagnosis<sup>11,152</sup> (► Table 2).

The HRCT patterns of both fibrotic and nonfibrotic HP rely on the detection of centrilobular nodules, mosaic attenuation, the three-density sign (previously known as the head cheese sign) on inspiratory HRCT, and lobular air trapping on expiration studies.<sup>11,13,153–156</sup> Additional features of fibrosis that are required to separate fibrotic HP from nonfibrotic HP include reticular or ground-glass opacities in association with traction bronchiectasis or bronchiolectasis, lobar volume loss, and honeycombing.

Centrilobular nodules in HP, characterized as nonbranching ground-glass nodules located in the center of the SPL, are more profuse in the nonfibrotic form of HP. The nodules are evenly spaced and do not touch the pleural and fissural surfaces or the interlobular septa. Distribution is diffuse in the axial plane, and either diffuse or upper and mid-zone predominant in the craniocaudal plane. Mosaic attenuation refers to sharply delineated, lobular, or subsegmental regions of different attenuation in the lung parenchyma.

**Table 2** Diagnostic CT categories of fibrotic HP based on CT patterns

HRCT	Typical fibrotic HP	Compatible with fibrotic HP	Indeterminate for fibrotic HP
Features	CT signs of fibrosis with either of the following: <ul style="list-style-type: none"> <li>• Profuse poorly defined centrilobular nodules of ground-glass opacity affecting all lung zones</li> <li>• Inspiratory mosaic attenuation with three-density sign.</li> <li>• Lack of features suggesting an alternative diagnosis</li> </ul>	CT signs of fibrosis with any of the following: <ul style="list-style-type: none"> <li>• Patchy or diffuse ground-glass opacity</li> <li>• Patchy, nonprofuse centrilobular nodules of ground-glass attenuation</li> <li>• Mosaic attenuation and lobular air-trapping that do not meet criteria for typical fibrotic HP</li> <li>• Lack of features suggesting an alternative diagnosis</li> </ul>	CT signs of fibrosis without other features suggestive of HP

Abbreviations: CT, computed tomography; HP, hypersensitivity pneumonitis; HRCT, high-resolution CT.

Notes: CT signs of fibrosis include any of the following: reticular or ground-glass abnormality with traction bronchiectasis or bronchiolectasis; lobar volume loss; honeycombing. The distribution of fibrotic HP is quite variable and often not diagnostically helpful. However, a mid-lung predominant distribution of fibrosis is suggestive of fibrotic HP, and an upper lobe predominance is much more common in fibrotic HP than in idiopathic pulmonary fibrosis.

Source: Adapted from Fernández Pérez et al.<sup>152</sup>

This document was downloaded for personal use only. Unauthorized distribution is strictly prohibited.

Increased attenuation, or ground-glass opacification, decreased attenuation and regions of normal attenuation are possible. The presence of all three attenuations, the “three-density sign” (formerly known as the head cheese sign),<sup>11,155</sup> is believed to be most specific for HP and allows differentiation from other ILDs, particularly NSIP and IPF.<sup>157</sup> When two attenuations are present, normal lung is adjacent to either increased attenuation or decreased attenuation. The latter shows persistence of decreased attenuation and lack of lobular volume reduction on expiration HRCT, secondary to lobular air trapping. In one study, fibrotic HP was more common than other fibrosing ILDs when diffuse distribution was present and mosaic attenuation and air trapping were more dominant than reticular opacity.<sup>143</sup> However, IPF may contain areas of air trapping within fibrotic regions, which can cause misdiagnosis. Barnett and colleagues identified lobular lucency of at least one lobule in three lobes and air trapping in IPF in more than 50 and 46% of cases, respectively.<sup>157</sup>

Only the ATS/JRS/ALAT guidelines utilize distribution of fibrotic changes in the lung to characterize cases as typical, compatible, or indeterminate for HP. Typical HP distribution includes diffuse, axial, or mid-zone predominant with sparing of the lung bases. Compatible HP distribution includes peribronchovascular, subpleural axial distribution and upper zone predominant. The Chest guidelines do not stratify patients by disease distribution since likelihood of disease does not change. Basal distribution occurs in HP in 30% and an upper zone distribution in 10 to 20% of cases, the remainder being diffuse or mid-zone.<sup>158–160</sup> Distribution can aid differentiation of HP from other fibrotic lung diseases, since upper or mid-zone distribution suggests HP rather than IPF.<sup>161,162</sup>

The “typical HP” HRCT findings of fibrotic HP are lung fibrosis coexisting with bronchiolar obstruction, manifesting as profuse poorly defined centrilobular nodules in the axial plane and inspiratory mosaic attenuation with the “three-density pattern” (► Fig. 22A, B).

The “compatible with HP” imaging findings are patchy or diffuse ground-glass opacity, nonprofuse centrilobular nodules, or mosaic attenuation and lobular air trapping that does not meet the typical fibrotic HP pattern (► Fig. 22C, D).

“Indeterminate of HP” findings include CT features of fibrosis that do not meet criteria for fibrotic HP.

Several studies have found that the use of histopathological findings and imaging patterns in combination characterize the severity and prognosis of fibrotic HP.<sup>25,163,164</sup> Specifically, the presence of subpleural and centriacinar fibroblastic foci (FF) in lung biopsies seen in parallel with increased extent of reticulation and traction bronchiectasis on imaging is associated with higher mortality rates.<sup>11,163–165</sup>

However, lung biopsies are infrequently performed in clinical practice,<sup>166</sup> which makes HRCT as a standalone tool indispensable in the diagnosis and management of fibrotic HP, particularly in the presence of an inciting antigen. Similarly, identification of traction bronchiectasis and evaluation of the extent of honeycombing has shown significant

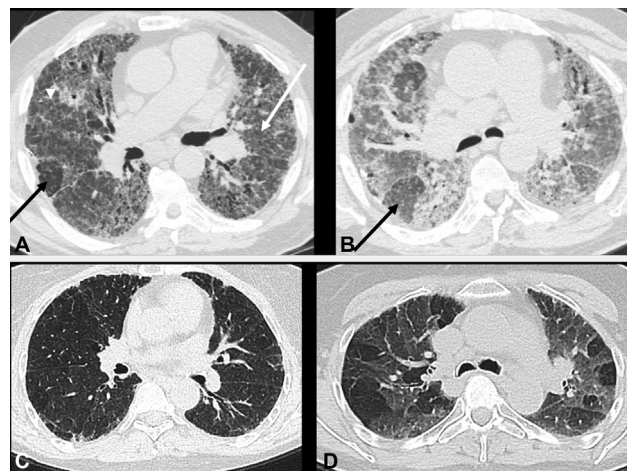


**Fig. 22** Typical fibrotic HP compatible with fibrotic HP. (A) Axial HRCT demonstrates centrilobular nodules (white arrow) and the three-density sign. There is ground-glass opacity, (asterisk), lobular low attenuation (black arrow), and normal lung (arrowhead). Fibrotic changes include subpleural reticulation and traction bronchiectasis. (B) Expiratory chest CT demonstrates air trapping (black arrow). Findings are typical for fibrotic hypersensitivity pneumonitis. (C) Axial HRCT demonstrates mosaic attenuation and subpleural reticulation. (D) Expiratory chest CT demonstrates lobular air trapping. Findings are compatible with fibrotic hypersensitivity pneumonitis.

advantages over pulmonary function tests for predicting mortality in patients with chronic disease.<sup>25</sup> Hansell et al found that areas of decreased attenuation on imaging are correlated with severity of air trapping, as indicated by residual volume ( $r = 0.58$ ,  $p < 0.01$ ), whereas ground-glass opacification and reticulation are correlated with restrictive lung function.<sup>153</sup>

The poor prognostic nature of fibrotic HP also appears to have ties to underlying genetic anomalies as well as other associated respiratory complications. A high prevalence of MUC5B promoter polymorphisms<sup>167</sup> and probands of familial pulmonary fibrosis are reported,<sup>168,169</sup> both of which have a significant impact on survival. Patients with fibrotic HP are also at a higher risk to develop other lung pathologies independent of smoking status,<sup>142,170,171</sup> such as combined pulmonary fibrosis and emphysema<sup>171</sup> and PPFE in combination with emphysema.<sup>170</sup>

## Conclusion

Careful evaluation of HRCT allows identification of abnormal features that indicate the presence of fibrosis. The common fibrotic ILDs have characteristic HRCT patterns, although there is often overlap. Multidisciplinary discussion that combines CT patterns with clinical, serologic, and pathologic can determine a working diagnosis and direct the most appropriate treatment. Recent updates of guidelines on diagnosis of IPF and new reclassification of HP provide a framework for further research and refinement.

## Conflict of Interest

None declared.

## References

- 1 Lynch DA, Sverzellati N, Travis WD, et al. Diagnostic criteria for idiopathic pulmonary fibrosis: a Fleischner Society White Paper. *Lancet Respir Med* 2018;6(02):138–153
- 2 Hodnett PA, Naidich DP. Fibrosing interstitial lung disease. A practical high-resolution computed tomography-based approach to diagnosis and management and a review of the literature. *Am J Respir Crit Care Med* 2013;188(02):141–149
- 3 American College of Radiology. ACR-STR Practice Parameter for the Performance of High-Resolution Computed Tomography (HRCT) of the Lungs in Adults. 2020. Accessed March 6, 2022, at: <https://www.acr.org/-/media/ACR/Files/Practice-Parameters/HRCT-Lungs.pdf>
- 4 American Thoracic Society European Respiratory Society. This joint statement of the American Thoracic Society (ATS), and the European Respiratory Society (ERS) was adopted by the ATS board of directors, June 2001 and by the ERS Executive Committee, June 2001. *Am J Respir Crit Care Med* 2002;165(02):277–304
- 5 Kishaba T. Acute exacerbation of idiopathic pulmonary fibrosis. *Medicina (Kaunas)* 2019;55(03):E70
- 6 Kim M, Lee SM, Song JW, et al. Added value of prone CT in the assessment of honeycombing and classification of usual interstitial pneumonia pattern. *Eur J Radiol* 2017;91:66–70
- 7 Verschakelen JA, Van fraeyenhoven L, Laureys G, Demedts M, Baert AL. Differences in CT density between dependent and nondependent portions of the lung: influence of lung volume. *AJR Am J Roentgenol* 1993;161(04):713–717
- 8 Lee KN, Yoon SK, Sohn CH, Choi PJ, Webb WR. Dependent lung opacity at thin-section CT: evaluation by spirometrically-gated CT of the influence of lung volume. *Korean J Radiol* 2002;3(01):24–29
- 9 Remy-Jardin M, Campistron P, Amara A, et al. Usefulness of coronal reformations in the diagnostic evaluation of infiltrative lung disease. *J Comput Assist Tomogr* 2003;27(02):266–273
- 10 Tokura S, Okuma T, Akira M, Arai T, Inoue Y, Kitaichi M. Utility of expiratory thin-section CT for fibrotic interstitial pneumonia. *Acta Radiol* 2014;55(09):1050–1055
- 11 Raghu G, Remy-Jardin M, Ryerson CJ, et al. Diagnosis of hypersensitivity pneumonitis in adults: an official ATS/JRS/ALAT clinical practice guideline. *Am J Respir Crit Care Med* 2020;202(03):e36–e69
- 12 Bhalla M, Naidich DP, McGuinness G, Gruden JF, Leitman BS, McCauley DI. Diffuse lung disease: assessment with helical CT—preliminary observations of the role of maximum and minimum intensity projection images. *Radiology* 1996;200(02):341–347
- 13 Hansell DM, Bankier AA, MacMahon H, McLoud TC, Müller NL, Remy J. Fleischner Society: glossary of terms for thoracic imaging. *Radiology* 2008;246(03):697–722
- 14 Oikonomou A, Prassopoulos P. Mimics in chest disease: interstitial opacities. *Insights Imaging* 2013;4(01):9–27
- 15 Webb WR. Thin-section CT of the secondary pulmonary lobule: anatomy and the image—the 2004 Fleischner lecture. *Radiology* 2006;239(02):322–338
- 16 Weibel ER. Fleischner Lecture. Looking into the lung: what can it tell us? *AJR Am J Roentgenol* 1979;133(06):1021–1031
- 17 Hatabu H, Hunninghake GM, Lynch DA. Interstitial lung abnormality: recognition and perspectives. *Radiology* 2019;291(01):1–3
- 18 Hochegger B, Marchiori E, Zanon M, et al. Imaging in idiopathic pulmonary fibrosis: diagnosis and mimics. *Clinics (São Paulo)* 2019;74:e225
- 19 Remy-Jardin M, Giraud F, Remy J, Copin MC, Gosselin B, Duhamel A. Importance of ground-glass attenuation in chronic diffuse infiltrative lung disease: pathologic-CT correlation. *Radiology* 1993;189(03):693–698
- 20 Suzuki Y, Saito J, Togawa R, Minemura H, Munakata M. Intralobular septal thickening on chest CT in a patient with pulmonary amyloidosis: a rare case study. *Thorax* 2017;72(07):673–674
- 21 Mai C, Verleden SE, McDonough JE, et al. Thin-section CT features of idiopathic pulmonary fibrosis correlated with micro-CT and histologic analysis. *Radiology* 2017;283(01):252–263
- 22 Mukhopadhyay S, Parambil JG. Acute interstitial pneumonia (AIP): relationship to Hamman-Rich syndrome, diffuse alveolar damage (DAD), and acute respiratory distress syndrome (ARDS). *Semin Respir Crit Care Med* 2012;33(05):476–485
- 23 Taniguchi H, Kondoh Y. Acute and subacute idiopathic interstitial pneumonias. *Respirology* 2016;21(05):810–820
- 24 Ichikado K. High-resolution computed tomography findings of acute respiratory distress syndrome, acute interstitial pneumonia, and acute exacerbation of idiopathic pulmonary fibrosis. *Semin Ultrasound CT MR* 2014;35(01):39–46
- 25 Walsh SL, Sverzellati N, Devaraj A, Wells AU, Hansell DM. Chronic hypersensitivity pneumonitis: high resolution computed tomography patterns and pulmonary function indices as prognostic determinants. *Eur Radiol* 2012;22(08):1672–1679
- 26 Walsh SL, Sverzellati N, Devaraj A, Keir GJ, Wells AU, Hansell DM. Connective tissue disease related fibrotic lung disease: high resolution computed tomographic and pulmonary function indices as prognostic determinants. *Thorax* 2014;69(03):216–222
- 27 Tominaga J, Bankier AA, Lee KS, et al; Study Group of Diffuse Interstitial Lung Disease in Japan. Inter-observer agreement in identifying traction bronchiectasis on computed tomography: its improvement with the use of the additional criteria for chronic fibrosing interstitial pneumonia. *Jpn J Radiol* 2019;37(11):773–780
- 28 Watadani T, Sakai F, Johkoh T, et al. Interobserver variability in the CT assessment of honeycombing in the lungs. *Radiology* 2013;266(03):936–944
- 29 Desai SR, Wells AU, Rubens MB, du Bois RM, Hansell DM. Traction bronchiectasis in cryptogenic fibrosing alveolitis: associated computed tomographic features and physiological significance. *Eur Radiol* 2003;13(08):1801–1808
- 30 Raghu G, Collard HR, Egan JJ, et al; ATS/ERS/JRS/ALAT Committee on Idiopathic Pulmonary Fibrosis. An official ATS/ERS/JRS/ALAT statement: idiopathic pulmonary fibrosis: evidence-based guidelines for diagnosis and management. *Am J Respir Crit Care Med* 2011;183(06):788–824
- 31 Westcott JL, Cole SR. Traction bronchiectasis in end-stage pulmonary fibrosis. *Radiology* 1986;161(03):665–669
- 32 Sundaram B, Gross BH, Martinez FJ, et al. Accuracy of high-resolution CT in the diagnosis of diffuse lung disease: effect of predominance and distribution of findings. *AJR Am J Roentgenol* 2008;191(04):1032–1039
- 33 Egashira R, Jacob J, Kokosi MA, et al. Diffuse pulmonary ossification in fibrosing interstitial lung diseases: prevalence and associations. *Radiology* 2017;284(01):255–263
- 34 Montag M. Radiographic Signs and Differential Diagnoses. In: Lange S, Walsh G, eds. *Radiology of Chest Diseases*. 3rd ed. Stuttgart: Thieme Verlagsgruppe; 2007:328–330
- 35 Chalmers JD, Goeminne P, Aliberti S, et al. The bronchiectasis severity index. An international derivation and validation study. *Am J Respir Crit Care Med* 2014;189(05):576–585
- 36 Matsuoka S, Uchiyama K, Shima H, Ueno N, Oishi S, Nojiri Y. Bronchoarterial ratio and bronchial wall thickness on high-resolution CT in asymptomatic subjects: correlation with age and smoking. *AJR Am J Roentgenol* 2003;180(02):513–518
- 37 Alhamad EH. Clinical characteristics and survival in idiopathic pulmonary fibrosis and connective tissue disease-associated usual interstitial pneumonia. *J Thorac Dis* 2015;7(03):386–393
- 38 Prenzel F, Harfst J, Schwerk N, et al; LIP/FB-Kids-Lung-Registry Study Group. Lymphocytic interstitial pneumonia and follicular

- bronchiolitis in children: a registry-based case series. *Pediatr Pulmonol* 2020;55(04):909–917
- 39 Flaherty KR, King TE Jr., Raghu G, et al. Idiopathic interstitial pneumonia: what is the effect of a multidisciplinary approach to diagnosis? *Am J Respir Crit Care Med* 2004;170(08):904–910
  - 40 Chaudhuri N, Spencer L, Greaves M, Bishop P, Chaturvedi A, Leonard C. A review of the multidisciplinary diagnosis of interstitial lung diseases: a retrospective analysis in a single UK specialist centre. *J Clin Med* 2016;5(08):E66
  - 41 Hobbs S, Chung JH, Leb J, Kaproth-Joslin K, Lynch DA. Practical imaging interpretation in patients suspected of having idiopathic pulmonary fibrosis: official recommendations from the Radiology Working Group of the Pulmonary Fibrosis Foundation. *Radiol Cardiothorac Imaging* 2021;3(01):e200279
  - 42 Raghu G, Remy-Jardin M, Myers JL, et al; American Thoracic Society, European Respiratory Society, Japanese Respiratory Society, and Latin American Thoracic Society. Diagnosis of idiopathic pulmonary fibrosis: an official ATS/ERS/JRS/ALAT clinical practice guideline. *Am J Respir Crit Care Med* 2018;198(05):e44–e68
  - 43 Madan R, Chansakul T, Goldberg HJ. Imaging in lung transplants: checklist for the radiologist. *Indian J Radiol Imaging* 2014;24(04):318–326
  - 44 Popper HH. Fibrosing pneumonia – how to diagnose, and how to recognize the etiology? *Surg Exp Pathol* 2020;3(15)
  - 45 Travis WD, Costabel U, Hansell DM, et al; ATS/ERS Committee on Idiopathic Interstitial Pneumonias. An official American Thoracic Society/European Respiratory Society statement: Update of the international multidisciplinary classification of the idiopathic interstitial pneumonias. *Am J Respir Crit Care Med* 2013;188(06):733–748
  - 46 Bonifazi M, Montero MA, Renzoni EA. Idiopathic pleuroparenchymal fibroelastosis. *Curr Pulmonol Rep* 2017;6(01):9–15
  - 47 Fell CD, Martinez FJ, Liu LX, et al. Clinical predictors of a diagnosis of idiopathic pulmonary fibrosis. *Am J Respir Crit Care Med* 2010;181(08):832–837
  - 48 Brownell R, Moua T, Henry TS, et al. The use of pretest probability increases the value of high-resolution CT in diagnosing usual interstitial pneumonia. *Thorax* 2017;72(05):424–429
  - 49 Shih AR, Nitiwarangkul C, Little BP, et al. Practical application and validation of the 2018 ATS/ERS/JRS/ALAT and Fleischner Society guidelines for the diagnosis of idiopathic pulmonary fibrosis. *Respir Res* 2021;22(01):124
  - 50 Yagihashi K, Huckleberry J, Colby TV, et al; Idiopathic Pulmonary Fibrosis Clinical Research Network (IPFnet) Radiologic-pathologic discordance in biopsy-proven usual interstitial pneumonia. *Eur Respir J* 2016;47(04):1189–1197
  - 51 Sumikawa H, Johkoh T, Colby TV, et al. Computed tomography findings in pathological usual interstitial pneumonia: relationship to survival. *Am J Respir Crit Care Med* 2008;177(04):433–439
  - 52 Sverzellati N, Wells AU, Tomassetti S, et al. Biopsy-proved idiopathic pulmonary fibrosis: spectrum of nondiagnostic thin-section CT diagnoses. *Radiology* 2010;254(03):957–964
  - 53 Raghu G, Lynch D, Godwin JD, et al. Diagnosis of idiopathic pulmonary fibrosis with high-resolution CT in patients with little or no radiological evidence of honeycombing: secondary analysis of a randomised, controlled trial. *Lancet Respir Med* 2014;2(04):277–284
  - 54 Chung JH, Chawla A, Peljto AL, et al. CT scan findings of probable usual interstitial pneumonitis have a high predictive value for histologic usual interstitial pneumonitis. *Chest* 2015;147(02):450–459
  - 55 Silva CI, Müller NL, Lynch DA, et al. Chronic hypersensitivity pneumonitis: differentiation from idiopathic pulmonary fibrosis and nonspecific interstitial pneumonia by using thin-section CT. *Radiology* 2008;246(01):288–297
  - 56 Flaherty KR, Thwaite EL, Kazerooni EA, et al. Radiological versus histological diagnosis in UIP and NSIP: survival implications. *Thorax* 2003;58(02):143–148
  - 57 Inomata M, Jo T, Kuse N, et al. Clinical impact of the radiological indeterminate for usual interstitial pneumonia pattern on the diagnosis of idiopathic pulmonary fibrosis. *Respir Investig* 2021;59(01):81–89
  - 58 Kwon BS, Choe J, Do KH, Hwang HS, Chae EJ, Song JW. Computed tomography patterns predict clinical course of idiopathic pulmonary fibrosis. *Respir Res* 2020;21(01):295
  - 59 Fukihara J, Kondoh Y, Brown KK, et al. Probable usual interstitial pneumonia pattern on chest CT: is it sufficient for a diagnosis of idiopathic pulmonary fibrosis? *Eur Respir J* 2020;55(04):1802465
  - 60 Salisbury ML, Tolle LB, Xia M, et al. Possible UIP pattern on high-resolution computed tomography is associated with better survival than definite UIP in IPF patients. *Respir Med* 2017;131:229–235
  - 61 Mononen ME, Kettunen HP, Suoranta SK, et al. Several specific high-resolution computed tomography patterns correlate with survival in patients with idiopathic pulmonary fibrosis. *J Thorac Dis* 2021;13(04):2319–2330
  - 62 Lee HY, Lee KS, Jeong YJ, et al. High-resolution CT findings in fibrotic idiopathic interstitial pneumonias with little honeycombing: serial changes and prognostic implications. *AJR Am J Roentgenol* 2012;199(05):982–989
  - 63 Salvatore M, Singh A, Yip R, et al. Progression of probable UIP and UIP on HRCT. *Clin Imaging* 2019;58(58):140–144
  - 64 Raghu G, Chen SY, Yeh WS, et al. Idiopathic pulmonary fibrosis in US Medicare beneficiaries aged 65 years and older: incidence, prevalence, and survival, 2001–11. *Lancet Respir Med* 2014;2(07):566–572
  - 65 Richeldi L, du Bois RM, Raghu G, et al; INPULSIS Trial Investigators. Efficacy and safety of nintedanib in idiopathic pulmonary fibrosis. *N Engl J Med* 2014;370(22):2071–2082
  - 66 King TE Jr., Bradford WZ, Castro-Bernardini S, et al; ASCEND Study Group. A phase 3 trial of pirfenidone in patients with idiopathic pulmonary fibrosis. *N Engl J Med* 2014;370(22):2083–2092
  - 67 Balestro E, Cocconcelli E, Giraudo C, et al. High-resolution CT change over time in patients with idiopathic pulmonary fibrosis on antifibrotic treatment. *J Clin Med* 2019;8(09):E1469
  - 68 Iwasawa T, Ogura T, Sakai F, et al. CT analysis of the effect of pirfenidone in patients with idiopathic pulmonary fibrosis. *Eur J Radiol* 2014;83(01):32–38
  - 69 Jacob J, Aksman L, Mogulkoc N, et al. Serial CT analysis in idiopathic pulmonary fibrosis: comparison of visual features that determine patient outcome. *Thorax* 2020;75(08):648–654
  - 70 Humphries SM, Yagihashi K, Huckleberry J, et al. Idiopathic pulmonary fibrosis: data-driven textural analysis of extent of fibrosis at baseline and 15-month follow-up. *Radiology* 2017;285(01):270–278
  - 71 Kligerman SJ, Groshong S, Brown KK, Lynch DA. Nonspecific interstitial pneumonia: radiologic, clinical, and pathologic considerations. *Radiographics* 2009;29(01):73–87
  - 72 Travis WD, Hunninghake G, King TE Jr., et al. Idiopathic nonspecific interstitial pneumonia: report of an American Thoracic Society project. *Am J Respir Crit Care Med* 2008;177(12):1338–1347
  - 73 Daniil ZD, Gilchrist FC, Nicholson AG, et al. A histologic pattern of nonspecific interstitial pneumonia is associated with a better prognosis than usual interstitial pneumonia in patients with cryptogenic fibrosing alveolitis. *Am J Respir Crit Care Med* 1999;160(03):899–905
  - 74 MacDonald SL, Rubens MB, Hansell DM, et al. Nonspecific interstitial pneumonia and usual interstitial pneumonia: comparative appearances at and diagnostic accuracy of thin-section CT. *Radiology* 2001;221(03):600–605

- 75 Lynch DA, Travis WD, Müller NL, et al. Idiopathic interstitial pneumonias: CT features. *Radiology* 2005;236(01):10–21
- 76 Ebner L, Christodoulidis S, Stathopoulou T, et al. Meta-analysis of the radiological and clinical features of usual interstitial pneumonia (UIP) and nonspecific interstitial pneumonia (NSIP). *PLoS One* 2020;15(01):e0226084
- 77 Katzenstein AL, Fiorelli RF. Nonspecific interstitial pneumonia/fibrosis. Histologic features and clinical significance. *Am J Surg Pathol* 1994;18(02):136–147
- 78 Silva CI, Müller NL, Hansell DM, Lee KS, Nicholson AG, Wells AU. Nonspecific interstitial pneumonia and idiopathic pulmonary fibrosis: changes in pattern and distribution of disease over time. *Radiology* 2008;247(01):251–259
- 79 Kim DS, Collard HR, King TE Jr. Classification and natural history of the idiopathic interstitial pneumonias. *Proc Am Thorac Soc* 2006;3(04):285–292
- 80 Akira M, Inoue G, Yamamoto S, Sakatani M. Non-specific interstitial pneumonia: findings on sequential CT scans of nine patients. *Thorax* 2000;55(10):854–859
- 81 Schneider F, Hwang DM, Gibson K, Yousem SA. Nonspecific interstitial pneumonia: a study of 6 patients with progressive disease. *Am J Surg Pathol* 2012;36(01):89–93
- 82 Enomoto N, Sumikawa H, Sugiura H, et al. Clinical, radiological, and pathological evaluation of “NSIP with OP overlap” pattern compared with NSIP in patients with idiopathic interstitial pneumonias. *Respir Med* 2020;174:106201
- 83 Jonigk D, Stark H, Braubach P, et al. Morphological and molecular motifs of fibrosing pulmonary injury patterns. *J Pathol Clin Res* 2019;5(04):256–271
- 84 BJORAKER JA, RYU JH, EDWIN MK, et al. Prognostic significance of histopathologic subsets in idiopathic pulmonary fibrosis. *Am J Respir Crit Care Med* 1998;157(01):199–203
- 85 Riha RL, Duhig EE, Clarke BE, Steele RH, Slaughter RE, Zimmerman PV. Survival of patients with biopsy-proven usual interstitial pneumonia and nonspecific interstitial pneumonia. *Eur Respir J* 2002;19(06):1114–1118
- 86 Flaherty KR, Toews GB, Travis WD, et al. Clinical significance of histological classification of idiopathic interstitial pneumonia. *Eur Respir J* 2002;19(02):275–283
- 87 Cottin V, Donsbeck AV, Revel D, Loire R, Cordier JF. Nonspecific interstitial pneumonia. Individualization of a clinicopathologic entity in a series of 12 patients. *Am J Respir Crit Care Med* 1998;158(04):1286–1293
- 88 Jain A, Shannon VR, Sheshadri A. Immune-related adverse events: pneumonitis. *Adv Exp Med Biol* 2018;995:131–149
- 89 Suda T, Kono M, Nakamura Y, et al. Distinct prognosis of idiopathic nonspecific interstitial pneumonia (NSIP) fulfilling criteria for undifferentiated connective tissue disease (UCTD). *Respir Med* 2010;104(10):1527–1534
- 90 Nunes H, Schubel K, Piver D, et al. Nonspecific interstitial pneumonia: survival is influenced by the underlying cause. *Eur Respir J* 2015;45(03):746–755
- 91 Latsi PI, du Bois RM, Nicholson AG, et al. Fibrotic idiopathic interstitial pneumonia: the prognostic value of longitudinal functional trends. *Am J Respir Crit Care Med* 2003;168(05):531–537
- 92 Jegal Y, Kim DS, Shim TS, et al. Physiology is a stronger predictor of survival than pathology in fibrotic interstitial pneumonia. *Am J Respir Crit Care Med* 2005;171(06):639–644
- 93 Tanizawa K, Handa T, Kubo T, et al. Clinical significance of radiological pleuroparenchymal fibroelastosis pattern in interstitial lung disease patients registered for lung transplantation: a retrospective cohort study. *Respir Res* 2018;19(01):162
- 94 Nunes H, Jeny F, Bouvry D, et al. Pleuroparenchymal fibroelastosis associated with telomerase reverse transcriptase mutations. *Eur Respir J* 2017;49(05):1602022
- 95 Pakhale SS, Hadjiliadis D, Howell DN, et al. Upper lobe fibrosis: a novel manifestation of chronic allograft dysfunction in lung transplantation. *J Heart Lung Transplant* 2005;24(09):1260–1268
- 96 von der Thüsen JH, Hansell DM, Tominaga M, et al. Pleuroparenchymal fibroelastosis in patients with pulmonary disease secondary to bone marrow transplantation. *Mod Pathol* 2011;24(12):1633–1639
- 97 Parish JM, Muhm JR, Leslie KO. Upper lobe pulmonary fibrosis associated with high-dose chemotherapy containing BCNU for bone marrow transplantation. *Mayo Clin Proc* 2003;78(05):630–634
- 98 Konen E, Weisbrod GL, Pakhale S, Chung T, Paul NS, Hutcheon MA. Fibrosis of the upper lobes: a newly identified late-onset complication after lung transplantation? *AJR Am J Roentgenol* 2003;181(06):1539–1543
- 99 Beynat-Mouterde C, Beltramo G, Lezmi G, et al. Pleuroparenchymal fibroelastosis as a late complication of chemotherapy agents. *Eur Respir J* 2014;44(02):523–527
- 100 Piciucchi S, Tomassetti S, Casoni G, et al. High resolution CT and histological findings in idiopathic pleuroparenchymal fibroelastosis: features and differential diagnosis. *Respir Res* 2011;12:111
- 101 Frankel SK, Cool CD, Lynch DA, Brown KK. Idiopathic pleuroparenchymal fibroelastosis: description of a novel clinicopathologic entity. *Chest* 2004;126(06):2007–2013
- 102 Morshid A, Moshksar A, Das A, Duarte AG, Palacio D, Villanueva-Meyer J. HRCT diagnosis of pleuroparenchymal fibroelastosis: report of two cases. *Radiol Case Rep* 2021;16(06):1564–1569
- 103 Fujisawa T, Horiike Y, Egashira R, et al. Radiological pleuroparenchymal fibroelastosis-like lesion in idiopathic interstitial pneumonias. *Respir Res* 2021;22(01):290
- 104 Esteves C, Costa FR, Redondo MT, et al. Pleuroparenchymal fibroelastosis: role of high-resolution computed tomography (HRCT) and CT-guided transthoracic core lung biopsy. *Insights Imaging* 2016;7(01):155–162
- 105 Reddy TL, Tominaga M, Hansell DM, et al. Pleuroparenchymal fibroelastosis: a spectrum of histopathological and imaging phenotypes. *Eur Respir J* 2012;40(02):377–385
- 106 Chua F, Desai SR, Nicholson AG, et al. Pleuroparenchymal fibroelastosis. A review of clinical, radiological, and pathological characteristics. *Ann Am Thorac Soc* 2019;16(11):1351–1359
- 107 Rasciti E, Cancellieri A, Romagnoli M, Dell’Amore A, Zompatori M. Suspected pleuroparenchymal fibroelastosis relapse after lung transplantation: a case report and literature review. *BJR Case Rep* 2019;5(04):20190040
- 108 Ofek E, Sato M, Saito T, et al. Restrictive allograft syndrome post lung transplantation is characterized by pleuroparenchymal fibroelastosis. *Mod Pathol* 2013;26(03):350–356
- 109 Bonham CA, Streck ME, Patterson KC. From granuloma to fibrosis: sarcoidosis associated pulmonary fibrosis. *Curr Opin Pulm Med* 2016;22(05):484–491
- 110 Handa T, Nagai S, Fushimi Y, et al. Clinical and radiographic indices associated with airflow limitation in patients with sarcoidosis. *Chest* 2006;130(06):1851–1856
- 111 Silva M, Nunes H, Valeyre D, Sverzellati N. Imaging of sarcoidosis. *Clin Rev Allergy Immunol* 2015;49(01):45–53
- 112 Polverosi R, Russo R, Coran A, et al. Typical and atypical pattern of pulmonary sarcoidosis at high-resolution CT: relation to clinical evolution and therapeutic procedures. *Radiol Med (Torino)* 2014;119(06):384–392
- 113 Tana C, Donatiello I, Coppola MG, et al. CT findings in pulmonary and abdominal sarcoidosis. Implications for diagnosis and classification. *J Clin Med* 2020;9(09):E3028
- 114 Sawahata M, Johkoh T, Kawanobe T, et al. Computed tomography images of fibrotic pulmonary sarcoidosis leading to chronic respiratory failure. *J Clin Med* 2020;9(01):E142
- 115 Nunes H, Uzunhan Y, Gille T, Lamberto C, Valeyre D, Brillet PY. Imaging of sarcoidosis of the airways and lung parenchyma and correlation with lung function. *Eur Respir J* 2012;40(03):750–765

- 116 Salvatore M, Toussie D, Pavlishyn N, et al. The right upper lobe bronchus angle: a tool for differentiating fibrotic and non-fibrotic sarcoidosis. *Sarcoidosis Vasc Diffuse Lung Dis* 2020;37(02):99–103
- 117 Verleden SE, Vanstapel A, De Sadeleer L, et al. Distinct airway involvement in subtypes of end-stage fibrotic pulmonary sarcoidosis. *Chest* 2021;160(02):562–571
- 118 Shigemitsu H, Oblad JM, Sharma OP, Koss MN. Chronic interstitial pneumonitis in end-stage sarcoidosis. *Eur Respir J* 2010;35(03):695–697
- 119 Zhang C, Chan KM, Schmidt LA, Myers JL. Histopathology of explanted lungs from patients with a diagnosis of pulmonary sarcoidosis. *Chest* 2016;149(02):499–507
- 120 Abehsera M, Valeyre D, Grenier P, Jaillet H, Battesti JP, Brauner MW. Sarcoidosis with pulmonary fibrosis: CT patterns and correlation with pulmonary function. *AJR Am J Roentgenol* 2000;174(06):1751–1757
- 121 Baughman RP, Engel PJ, Taylor L, Lower EE. Survival in sarcoidosis-associated pulmonary hypertension: the importance of hemodynamic evaluation. *Chest* 2010;138(05):1078–1085
- 122 Diaz-Guzman E, Farver C, Parambil J, Culver DA. Pulmonary hypertension caused by sarcoidosis. *Clin Chest Med* 2008;29(03):549–563, x
- 123 Spagnolo P, Rossi G, Trisolini R, Sverzellati N, Baughman RP, Wells AU. Pulmonary sarcoidosis. *Lancet Respir Med* 2018;6(05):389–402
- 124 Walsh SL, Wells AU, Sverzellati N, et al. An integrated clinicoradiological staging system for pulmonary sarcoidosis: a case-cohort study. *Lancet Respir Med* 2014;2(02):123–130
- 125 Hoffstein V, Ranganathan N, Mullen JB. Sarcoidosis simulating pulmonary veno-occlusive disease. *Am Rev Respir Dis* 1986;134(04):809–811
- 126 Hanak V, Golbin JM, Ryu JH. Causes and presenting features in 85 consecutive patients with hypersensitivity pneumonitis. *Mayo Clin Proc* 2007;82(07):812–816
- 127 Fernández Pérez ER, Swigris JJ, Forssén AV, et al. Identifying an inciting antigen is associated with improved survival in patients with chronic hypersensitivity pneumonitis. *Chest* 2013;144(05):1644–1651
- 128 Inase N, Ohtani Y, Sumi Y, et al. A clinical study of hypersensitivity pneumonitis presumably caused by feather duvets. *Ann Allergy Asthma Immunol* 2006;96(01):98–104
- 129 Jordan LE, Guy E. Paediatric feather duvet hypersensitivity pneumonitis. *BMJ Case Rep* 2015;2015:bcr2014207956
- 130 Ryerson CJ, Vittinghoff E, Ley B, et al. Predicting survival across chronic interstitial lung disease: the ILD-GAP model. *Chest* 2014;145(04):723–728
- 131 Morell F, Roger À, Reyes L, Cruz MJ, Murio C, Muñoz X. Bird fancier's lung: a series of 86 patients. *Medicine (Baltimore)* 2008;87(02):110–130
- 132 Thomeer MJ, Costabe U, Rizzato G, Poletti V, Demedts M. Comparison of registries of interstitial lung diseases in three European countries. *Eur Respir J Suppl* 2001;32:114s–118s
- 133 Schweisfurth H. Report by the Scientific Working Group for Therapy of Lung Diseases: German Fibrosis Register with initial results. *Pneumologie* 1996;50(12):899–901 [Mitteilung der Wissenschaftlichen Arbeitsgemeinschaft für die Therapie von Lungenkrankheiten (WATL): Deutsches Fibroseregister mit ersten Ergebnissen]
- 134 Thomeer M, Demedts M, Vandeurzen KVRGT Working Group on Interstitial Lung Diseases. Registration of interstitial lung diseases by 20 centres of respiratory medicine in Flanders. *Acta Clin Belg* 2001;56(03):163–172
- 135 Fisher JH, Kolb M, Algami M, et al. Baseline characteristics and comorbidities in the CAnadian Registry for Pulmonary Fibrosis. *BMC Pulm Med* 2019;19(01):223
- 136 Kreuter M, Herth FJ, Wacker M, et al. Exploring clinical and epidemiological characteristics of interstitial lung diseases: rationale, aims, and design of a nationwide prospective registry – the EXCITING-ILD Registry. *BioMed Res Int* 2015;2015:123876
- 137 Karakatsani A, Papakosta D, Rapti A, et al; Hellenic Interstitial Lung Diseases Group. Epidemiology of interstitial lung diseases in Greece. *Respir Med* 2009;103(08):1122–1129
- 138 Ansarie M. A national guideline and ILD PAK Registry Report: recent landmarks in the understanding of interstitial lung diseases in Pakistan. *J Pak Med Assoc* 2016;66(09):1050–1053
- 139 Strâmbu I. REGIS–Romanian National Registry for Interstitial Lung Diseases and Sarcoidosis: launch of the website and building-up the database. *Pneumologia* 2014;63(02):96–99 [REGIS–Registrul Național de Pneumopatii Interstițiale Difuze și Sarcoidoză: lansarea site-ului web și modul de alcătuire a bazei de date]
- 140 Singh S, Collins BF, Sharma BB, et al. Interstitial lung disease in India. Results of a prospective registry. *Am J Respir Crit Care Med* 2017;195(06):801–813
- 141 Singh S, Collins BF, Sharma BB, et al. Hypersensitivity pneumonitis: clinical manifestations - prospective data from the interstitial lung disease-India registry. *Lung India* 2019;36(06):476–482
- 142 Seed MJ, Agius RM. Progress with structure-activity relationship modelling of occupational chemical respiratory sensitizers. *Curr Opin Allergy Clin Immunol* 2017;17(02):64–71
- 143 Salisbury ML, Gross BH, Chughtai A, et al. Development and validation of a radiological diagnosis model for hypersensitivity pneumonitis. *Eur Respir J* 2018;52(02):1800443
- 144 Lalancette M, Carrier G, Laviolette M, et al. Farmer's lung. Long-term outcome and lack of predictive value of bronchoalveolar lavage fibrosing factors. *Am Rev Respir Dis* 1993;148(01):216–221
- 145 Baqir M, White D, Ryu JH. Emphysematous changes in hypersensitivity pneumonitis: a retrospective analysis of 12 patients. *Respir Med Case Rep* 2018;24:25–29
- 146 Miyazaki Y, Tateishi T, Akashi T, Ohtani Y, Inase N, Yoshizawa Y. Clinical predictors and histologic appearance of acute exacerbations in chronic hypersensitivity pneumonitis. *Chest* 2008;134(06):1265–1270
- 147 Fink JN, Ortega HG, Reynolds HY, et al. Needs and opportunities for research in hypersensitivity pneumonitis. *Am J Respir Crit Care Med* 2005;171(07):792–798
- 148 Richerson HB, Bernstein IL, Fink JN, et al. Guidelines for the clinical evaluation of hypersensitivity pneumonitis. Report of the Subcommittee on Hypersensitivity Pneumonitis. *J Allergy Clin Immunol* 1989;84(5, Pt 2):839–844
- 149 Fernández Pérez ER, Kong AM, Raimundo K, Koelsch TL, Kulkarni R, Cole AL. Epidemiology of hypersensitivity pneumonitis among an insured population in the United States: a claims-based cohort analysis. *Ann Am Thorac Soc* 2018;15(04):460–469
- 150 Wells AU, Flaherty KR, Brown KK, et al; INBUILD trial investigators. Nintedanib in patients with progressive fibrosing interstitial lung diseases-subgroup analyses by interstitial lung disease diagnosis in the INBUILD trial: a randomised, double-blind, placebo-controlled, parallel-group trial. *Lancet Respir Med* 2020;8(05):453–460
- 151 Wang BR, Edwards R, Freiheit EA, et al. The Pulmonary Fibrosis Foundation Patient Registry. Rationale, design, and methods. *Ann Am Thorac Soc* 2020;17(12):1620–1628
- 152 Fernández Pérez ER, Travis WD, Lynch DA, et al. Diagnosis and evaluation of hypersensitivity pneumonitis: CHEST Guideline and Expert Panel Report. *Chest* 2021;160(02):e97–e156
- 153 Hansell DM, Wells AU, Padley SP, Müller NL. Hypersensitivity pneumonitis: correlation of individual CT patterns with functional abnormalities. *Radiology* 1996;199(01):123–128

- 154 Okada F, Ando Y, Yoshitake S, et al. Clinical/pathologic correlations in 553 patients with primary centrilobular findings on high-resolution CT scan of the thorax. *Chest* 2007;132(06):1939–1948
- 155 Chung MH, Edinburgh KJ, Webb EM, McCowin M, Webb WR. Mixed infiltrative and obstructive disease on high-resolution CT: differential diagnosis and functional correlates in a consecutive series. *J Thorac Imaging* 2001;16(02):69–75
- 156 Morisset J, Johannson KA, Jones KD, et al; HP Delphi Collaborators. Identification of diagnostic criteria for chronic hypersensitivity pneumonitis: an international modified Delphi survey. *Am J Respir Crit Care Med* 2018;197(08):1036–1044
- 157 Barnett J, Molyneaux PL, Rawal B, et al. Variable utility of mosaic attenuation to distinguish fibrotic hypersensitivity pneumonitis from idiopathic pulmonary fibrosis. *Eur Respir J* 2019;54(01):1900531
- 158 Chung JH, Zhan X, Cao M, et al. Presence of air trapping and mosaic attenuation on chest computed tomography predicts survival in chronic hypersensitivity pneumonitis. *Ann Am Thorac Soc* 2017;14(10):1533–1538
- 159 Salisbury ML, Gu T, Murray S, et al. Hypersensitivity pneumonitis: radiologic phenotypes are associated with distinct survival time and pulmonary function trajectory. *Chest* 2019;155(04):699–711
- 160 Chung JH, Montner SM, Adegunsoye A, et al. CT findings associated with survival in chronic hypersensitivity pneumonitis. *Eur Radiol* 2017;27(12):5127–5135
- 161 Lynch DA, Newell JD, Logan PM, King TE Jr., Müller NL. Can CT distinguish hypersensitivity pneumonitis from idiopathic pulmonary fibrosis? *AJR Am J Roentgenol* 1995;165(04):807–811
- 162 Adler BD, Padley SP, Müller NL, Remy-Jardin M, Remy J. Chronic hypersensitivity pneumonitis: high-resolution CT and radiographic features in 16 patients. *Radiology* 1992;185(01):91–95
- 163 Walsh SL, Wells AU, Sverzellati N, et al. Relationship between fibroblastic foci profusion and high resolution CT morphology in fibrotic lung disease. *BMC Med* 2015;13:241
- 164 Sahin H, Brown KK, Curran-Everett D, et al. Chronic hypersensitivity pneumonitis: CT features comparison with pathologic evidence of fibrosis and survival. *Radiology* 2007;244(02):591–598
- 165 Chiba S, Tsuchiya K, Akashi T, et al. Chronic hypersensitivity pneumonitis with a usual interstitial pneumonia-like pattern: correlation between histopathologic and clinical findings. *Chest* 2016;149(06):1473–1481
- 166 Buendia-Roldan I, Aguilar-Duran H, Johannson KA, Selman M. Comparing the performance of two recommended criteria for establishing a diagnosis for hypersensitivity pneumonitis. *Am J Respir Crit Care Med* 2021;204(07):865–868
- 167 Ley B, Newton CA, Arnould I, et al. The MUC5B promoter polymorphism and telomere length in patients with chronic hypersensitivity pneumonitis: an observational cohort-control study. *Lancet Respir Med* 2017;5(08):639–647
- 168 Newton CA, Batra K, Torrealba J, et al. Telomere-related lung fibrosis is diagnostically heterogeneous but uniformly progressive. *Eur Respir J* 2016;48(06):1710–1720
- 169 Okamoto T, Miyazaki Y, Tomita M, Tamaoka M, Inase N. A familial history of pulmonary fibrosis in patients with chronic hypersensitivity pneumonitis. *Respiration* 2013;85(05):384–390
- 170 Jacob J, Odink A, Brun AL, et al. Functional associations of pleuroparenchymal fibroelastosis and emphysema with hypersensitivity pneumonitis. *Respir Med* 2018;138:95–101
- 171 Soumagne T, Chardon ML, Dournes G, et al. Emphysema in active farmer's lung disease. *PLoS One* 2017;12(06):e0178263